RSC Advances

PAPER

View Article Online
View Journal | View Issue

Cite this: *RSC Adv.*, 2022, **12**, 22503

Diclofenac derivatives as concomitant inhibitors of cholinesterase, monoamine oxidase, cyclooxygenase-2 and 5-lipoxygenase for the treatment of Alzheimer's disease: synthesis, pharmacology, toxicity and docking studies†

Muhammad Aamir Javed,[a] Saba Bibi,[a] Muhammad Saeed Jan,[b] Muhammad Ikram,[c] Asma Zaidi,[a] Umar Farooq,[a] Abdul Sadiq*[d] and Umer Rashid*[a]

Targeting concomitantly cholinesterase (ChEs) and monoamine oxidases (MAO-A and MAO-B) is a key strategy to treat multifactorial Alzheimer's disease (AD). Moreover, it is reported that the expression of cyclooxygenase-2 (COX-2) and lipoxygenase (LOX) is increased significantly in the brain of AD patients. Using the triazole of diclofenac **12** as a lead compound, we synthesized a variety of analogs as multipotent inhibitors concomitantly targeting COX-2, 5-LOX, AChE, BChE, MAO-A and MAO-B. A number of compounds showed excellent *in vitro* inhibition of the target biological macromolecules in nanomolar concentration. Compound **39** emerged as the most potent multitarget ligand with IC_{50} values of 0.03 μM, 0.91 μM, 0.61 μM, 0.01 μM 0.60 μM and 0.98 μM towards AChE, BChE, MAO-A, MAO-B, COX-2 and 5-LOX respectively. All the biologically active compounds were found to be non-neurotoxic and blood–brain barrier penetrant by using PAMPA assay. In a reversibility assay, all the studied active compounds showed reversibility and thus were found to be devoid of side effects. MTT assay results on neuroblastoma SH-SY5Y cells showed that the tested compounds were non-neurotoxic. An *in vivo* acute toxicity study showed the safety of the synthesized compounds up to a 2000 mg kg^{-1} dose. In docking studies three-dimensional construction and interaction with key residues of all the studied biological macromolecules helped us to explain the experimental results.

Received 6th July 2022
Accepted 3rd August 2022

DOI: 10.1039/d2ra04183a

rsc.li/rsc-advances

1 Introduction

Alzheimer's disease (AD) is a progressive neurological age-related disorder that begins slowly, worsens with time, and causes loss of memory as well as cognitive impairments. Formation of neurofibrillary tangles and free radicals, oxidative stress, excessive beta-amyloid peptide accumulation, irregular bio metal homeostasis, dystrophic neurites, dysfunctional microglia, reactive astrocytes, and reduced cholinergic functions are all pathological factors that contribute to the onset and progression of disease.[1–4] It primarily affects persons over the age of 65, and it is caused by a lack of acetylcholine (ACh), a neurotransmitter, in the neocortex and hippocampus. As a result, AD is marked by severe cholinergic neuron damage and decreased cholinergic functioning.[5,6] Increasing evidence revealed that pathologically AD is not only confined to the neuronal dysfunction but is also associated with the immunological processes of the brain which triggers the secretion of proinflammatory agents, involved in the development and severity of disease.[7,8] Neuroinflammation (NI) is a defensive mechanism in the brain that develops in response to neuronal stress and has been associated to a variety of chronic neurodegenerative diseases, including Alzheimer's disease. Toxins, infections, and certain medicines can all induce NI. Glia cells in the brain, such as microglia and astroglia, create proinflammatory mediators such cytokines and chemokines, that trigger neuroinflammatory processes.[9–11]

COX-1 is expressed in the brain on a constant basis, but COX-2 expression in neurons and glial cells is increased in neurodegenerative disorders. COX-2 is an enzyme that converts arachidonic acid to prostaglandins, that are important inflammatory mediators. COX-2-produced prostaglandins such as PGD2, PGE2, and PGJ2 have been found to increase in the frontal cortex of Alzheimer's disease patients, coupled with

[a]*Department of Chemistry, COMSATS University Islamabad, Abbottabad Campus, 22060 Abbottabad, Pakistan. E-mail: umerrashid@cuiatd.edu.pk*
[b]*Department of Pharmacy, University of Swabi, Swabi, 23430, KP, Pakistan*
[c]*Department of Pharmacy, COMSATS University Islamabad, Abbottabad Campus, 22060 Abbottabad, Pakistan*
[d]*Department of Pharmacy, Faculty of Biological Sciences, University of Malakand, Chakdara, 18000 Dir (L), KP, Pakistan. E-mail: sadiquom@yahoo.com*

† Electronic supplementary information (ESI) available. See https://doi.org/10.1039/d2ra04183a

microglia and astrocyte activation in senile plaques. Inhibition of COX-2 can help to alleviate inflammation and pain symptoms. COX-2 expression is dramatically enhanced in the brains of AD patients. COX-2 inhibitors could thus be beneficial in the treatment of neurological diseases.[5,12,13]

LOX-5 is a central nervous system enzyme that catalyzes the conversion of arachidonic acid to leukotrienes. It was also discovered that LOX-5 inhibitors can protect against β-amyloid mediated neurotoxicity. The AD brain has a higher amount of lipoxygenase (LOX) expression, which has been linked to increased Aβ production and tau phosphorylation. Studies on animal models have shown that 5- or 12- or 15-LOX inhibitors can reduce β-amyloid and tau pathology while also improving cognitive impairment. Experiments have also indicated a relationship between oxidative stress and LOXs and their metabolites in Alzheimer's patients. These data suggest that LOX-5 could be a promising target for future anti-NI medicines.[14,15]

Furthermore, nonsteroidal anti-inflammatory medications (NSAIDs) have been demonstrated to have protective benefits in lowering or delaying the progression of Alzheimer's disease in various epidemiologic and observational investigations. Randomized controlled trials, on the other hand, refute this theory. This discrepancy could be owing to the disease's multidimensional character and/or a failure to choose a proper cohort of patients, or due to a lack of relevant biomarkers for accurate patient stratification, or due to a lack of appropriate biomarkers.[16] Another essential enzyme associated with the etiology of AD is MAO, a vital flavoenzyme, which has two isoforms, MAO-A and MAO-B. MAO-B is involved in the metabolism of dopamine and performs a vital function in oxidative stress as it alters the redox state of glial cells and neurons. MAO-B expression is shown to be much higher in the hippocampus and cerebral cortex of Alzheimer's patients, accompanied with an excess of reactive oxygen species and hydrogen peroxide.[17–19] AD is currently untreatable and presently available anti-cholinesterase FDA approved drugs like donepezil, rivastigmine, galantamine and memantine, are single-target drugs that improve memory loss and cognitive functions whereas these are unable to completely cure dementia. In AD several relevant targets in various cell signaling pathways interact to form a network, thus making it difficult for single target drugs to cure the disease effectively. Therefore, multi-target strategies are being adopted to regulate the disease progression.[20–23] In designing MTDLs, to obtain maximum efficiency and superior outcomes for the treatment of AD, cholinesterase inhibitors are used to reduce the expression of AChE which is also accompanied by controlling other disease modifying factors which are involved in pathogenesis of AD.[4]

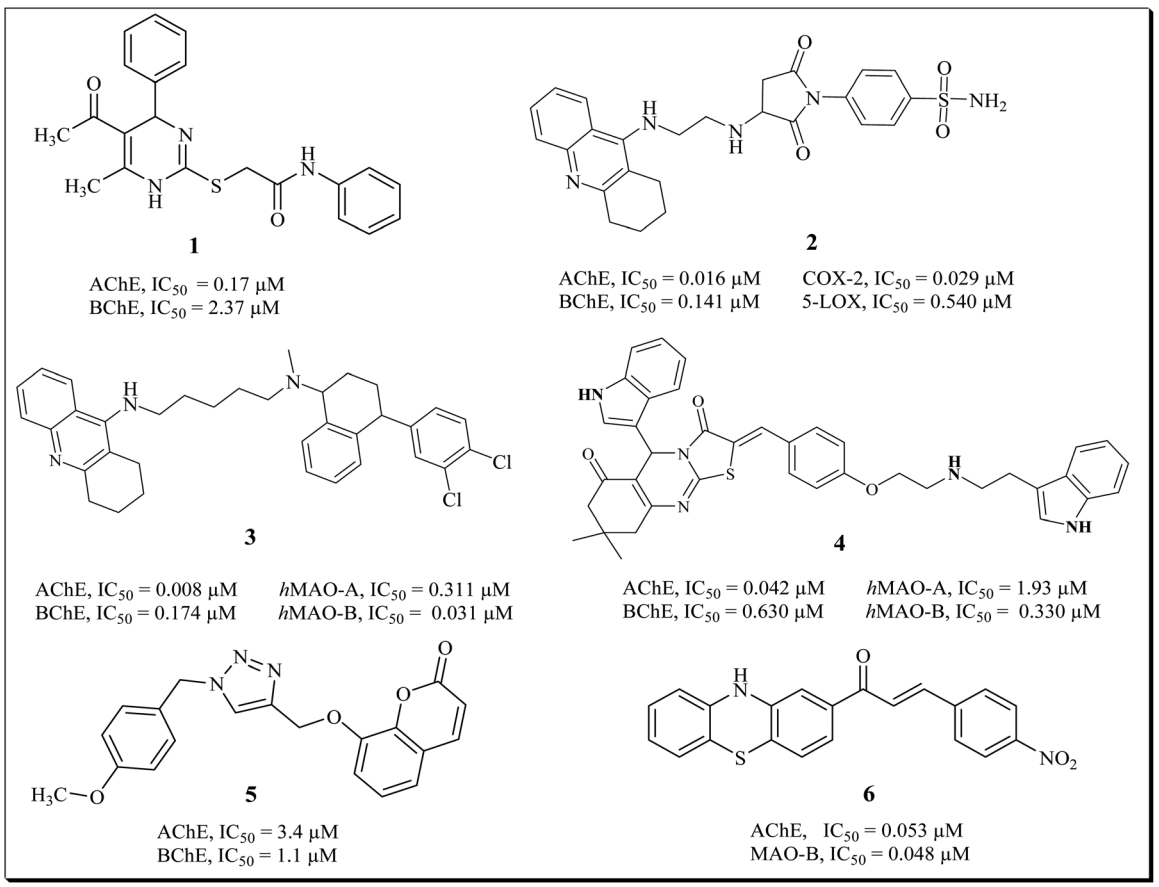

Fig. 1 Structures of some reported multitargeted compounds.

Our research group previously synthesized pharmacological vital pyrimidine based dual binding site concomitant inhibitors for AChE and BChE. Compound (**1**) exhibited inhibition potential of 0.17 μM and 2.37 μM for AChE and BChE.[24] We recently reported the pyrrolidine-sulfonamide derivative as potent multitarget inhibitors for the treatment of cholinergic deficit and neuroinflammation in AD. The potent compounds (**2**) showed inhibition of COX-2, 5-LOX, AChE and BChE in nano molar range.[5] Tacrine-sertraline derivative (**3**) emerged as the most potent inhibitor of AChE, BChE, MAO-A and MAO-B with IC_{50} values of 0.008 μM, 0.174 μM, 0.311 and 0.031 μM respectively.[25] We also reported thiazolidine derivatives as potent multi target inhibitor for treatment of AD. Compound (**4**) exhibits potential inhibition of AChE, BChE, MAO-A, MAO-B with IC_{50} of 0.042 μM, 0.630 μM, 1.93 μM and 0.33 μM respectively.[26] Askarani *et al.*, reported triazole based chromenone derivatives as multitarget inhibitor for treatment of AD, the potent inhibitor (**5**) showed IC_{50} of 3.4 μM (AChE) and 1.1 μM (BChE).[27] Yamali *et al.*, reported phenothiazine based chalcones as AChE/BChE and MAO-A/MAO-B inhibitors *via* base catalyzed Claisen Schmidt condensation reaction. The potent compound (**6**) presented excellent inhibition of AChE and MAO-B with IC_{50} of 0.053 ± 0.001 μM and 0.048 ± 0.001 μM respectively (Fig. 1).[28]

2 Results and discussion

2.1 Design strategy

Diclofenac is considered as an important anti-inflammatory agent. The presence of phenylacetic acid, secondary amine and a phenyl ring with two chloro-groups at *ortho*-position make it widely used for structural modification. In current study, we decided to modify the diclofenac structure to obtain compounds with multiple targeting properties related to AD including neuroinflammation. As described in Introduction section, previous reports from our laboratory identified pyrrolidine, pyrimidine and sulfonamide structural motifs endowed with multitarget inhibition for the treatment of AD. Moreover, it is also identified that the volume of active sites of AChE/BChE and MAO isoforms support bulky compounds for excellent inhibition. In current research, the bulk of the compounds were increased by the incorporation of various rigid (triazole, pyrazoline) and flexible (alkyl) linkers. Hydrophobic moieties such as phenyl rings, bicyclic (pyrimidine) and tricyclic fused ring systems (phenothiazine) at one or at both ends of the molecules to enhance the interactions with hydrophobic Trp279 and Trp84 (TcAChE numbering). In our previous reports, incorporation of pyrrolidine 2,5-dione framework showed multitarget anti-inflammatory and anti-Alzheimer activities. Hence, we also

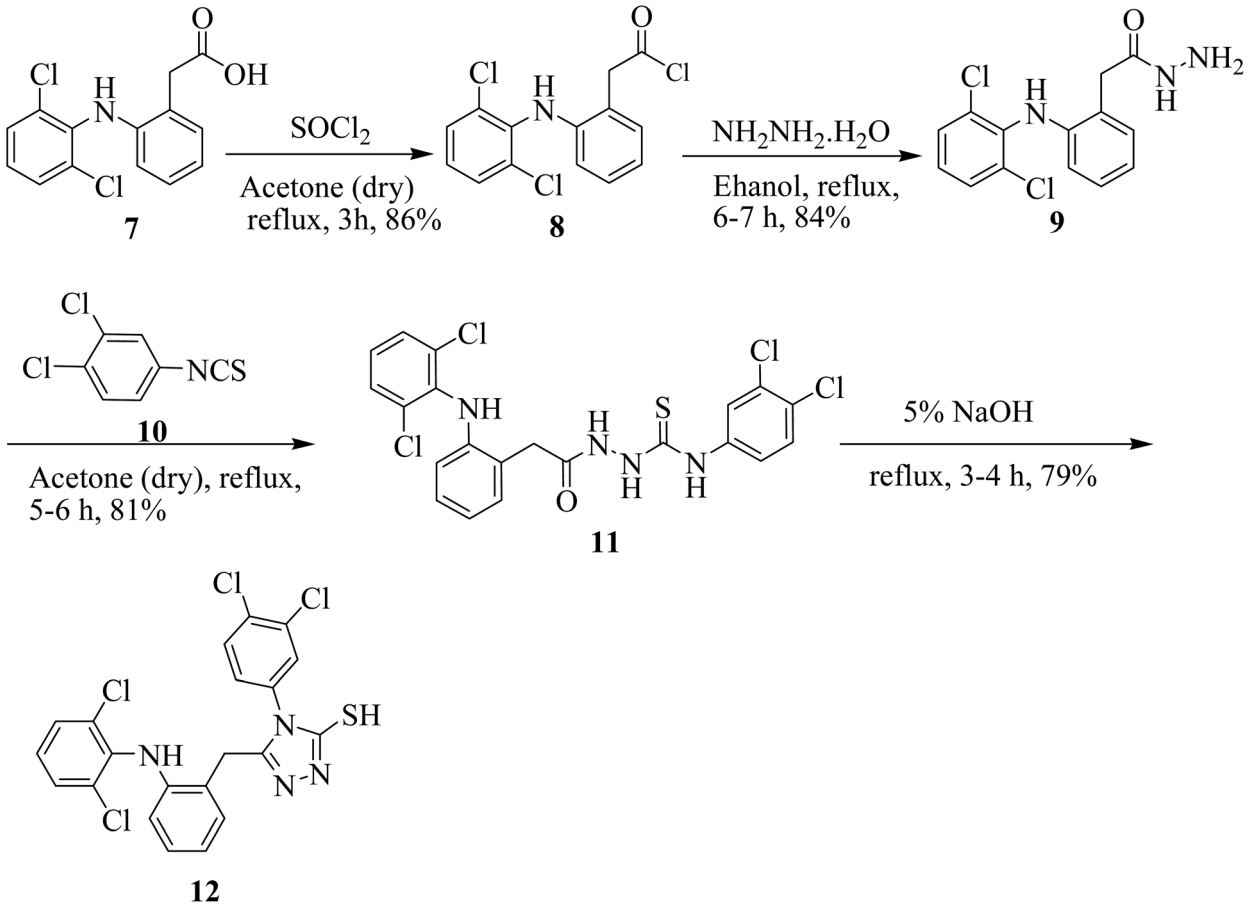

Scheme 1 Synthesis of triazole analog **12**.

decide to incorporate this framework to enhance the multi-target inhibition.

2.2 Chemistry

The synthesis of 5-(2-(2,6-dichlorophenylamino) benzyl)-4-(3,4-dichlorophenyl)-4*H*-1,2,4-triazole-3-thiol (**12**) is illustrated in Scheme 1. Acyl halide of diclofenac acid was synthesized by using thionyl chloride in dry acetone. The synthesized derivative was further treated with hydrazine hydrate in the presence of absolute ethanol to obtain 2-(2-(2,6-dichlorophenylamino) phenyl)acetohydrazide **9**. Further, hydrazide **9** on treatment with 1,2-dichloro-4-isothiocyanatobenzene (**10**) in dry acetone gave thiosemicarbazide derivative **11**. The synthesized thiosemicarbazide 11 when treated with 5% NaOH solution, produced target compound **12** (Scheme 1).

A synthetic strategy in hand allowed us to explore the SAR of 5-substituted-phenyl-4*H*-1,2,4-triazole-3-thiol derivative compound **15**. First, we synthesized Mannich base by the reaction of 3-thiol, formaldehyde and sulfanilamide in methanol under reflux conditions (Scheme 2).

Furthermore, we synthesized derivative of **12** with thiols and secondary amines (R-XH, **18–25**) having four methylene units. Compound **12** was treated with 1,4-dibromo butane in the presence of TEA in dichloromethane (DCM) as solvent. The synthesized intermediate was further reacted with dihydropyrimidine-2-thiones (**18–22**), succinimide derivatives **23**, **24** and tricyclic phenothiazine **25** to obtain the target compounds **26–33** (Scheme 3).

Subsequently, we synthesized the pyrazoline based sulfonamide derivative **39** of diclofenac acid by following a multi-steps protocol. In the first step, 4-aminoacetophenone (**34**), was coupled with diclofenac acid by using (DCC/DMAP) to obtain amide (**35**). The amide intermediate was then reacted with 4-chlorobenzaldehyde (**36**) to form chalcone derivative **37**. The chalcone based compound (**37**) finally treated with 4-hydrazinylbenzenesulfonamide (**38**) in the presence of base NaOH and stir in ethanol at room temperature for 2 h and obtained pyrazoline based compound **39** (Scheme 4).

2.3 *In vitro* pharmacology

Diclofenac is a non-selective NSAID used for the inhibition of cyclooxygenase (COX) as a pain reliever. In current study, we modified the diclofenac structure to obtain compounds with multiple targeting properties related to AD including neuroinflammation. The standard reported literature screening assay procedures were used for all inhibition bioassays. The inhibitory activities of the synthesized derivatives toward macromolecules inhibition are listed in Tables 1 and 2. Diclofenac sodium, celecoxib, zileuton, donepezil and safinamide were used as reference drugs. Conversion of 4-phenylthiosemicarbazide (**11**) to 1,2,4-triazole-3-thiol (**12**) was inspired by the typical 1,2-disubstituted pattern of celecoxib like selective COX-2 inhibitors. Interestingly as per our expectations, 1,2,4-triazole-3-thiol (**12**) showed improved COX-2 inhibition profile (IC_{50} = 0.69 μM) better than reference diclofenac (Table 1). However, as compared with triazole **12**, intermediate thiosemicarbazide derivative (**11**) showed good inhibition toward eeAChE, eqBChE, MAO-A and MAO-B (Table 2). Continued with triazole **12** as lead compound, we modified it by considering the 3D structures of macromolecules. Synthesis of Mannich base **15** containing sulfonamide moiety exhibited improved COX-2 and 5-LOX inhibition compared to lead **12** (Table 1). Incorporation of 3-methylene unit linker and pyrimidine/pyrrolidine/phenothiazine cores resulted in no inhibition of COX-2 in tested

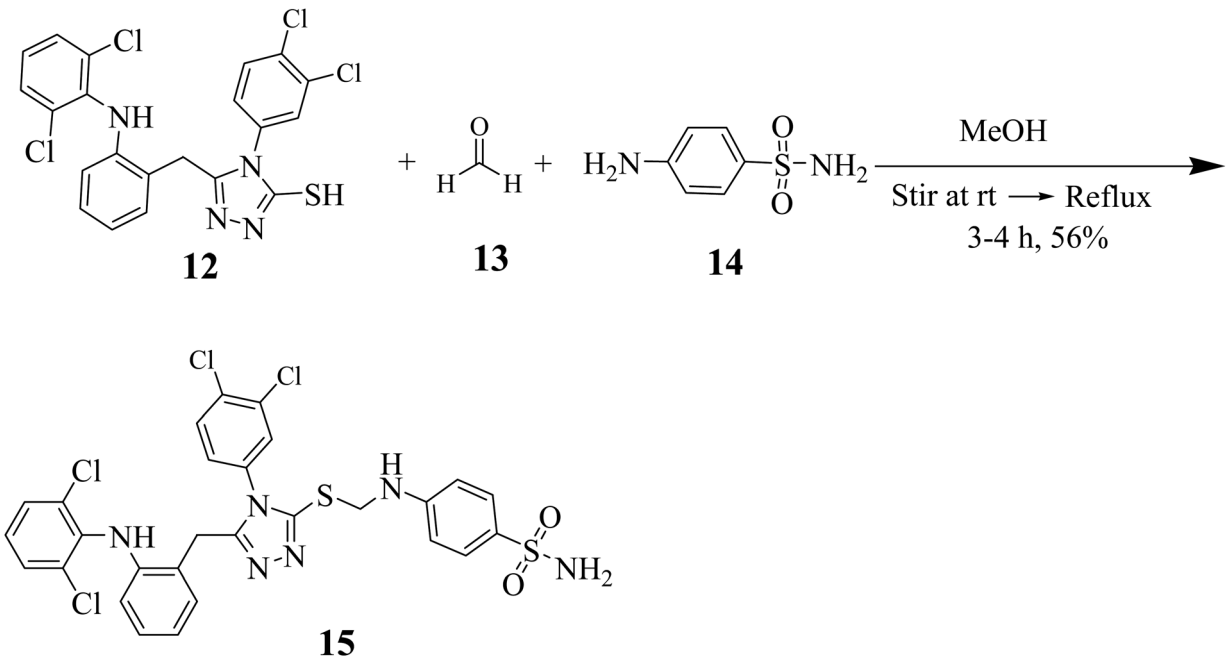

Scheme 2 Synthesis of Mannich base **15**.

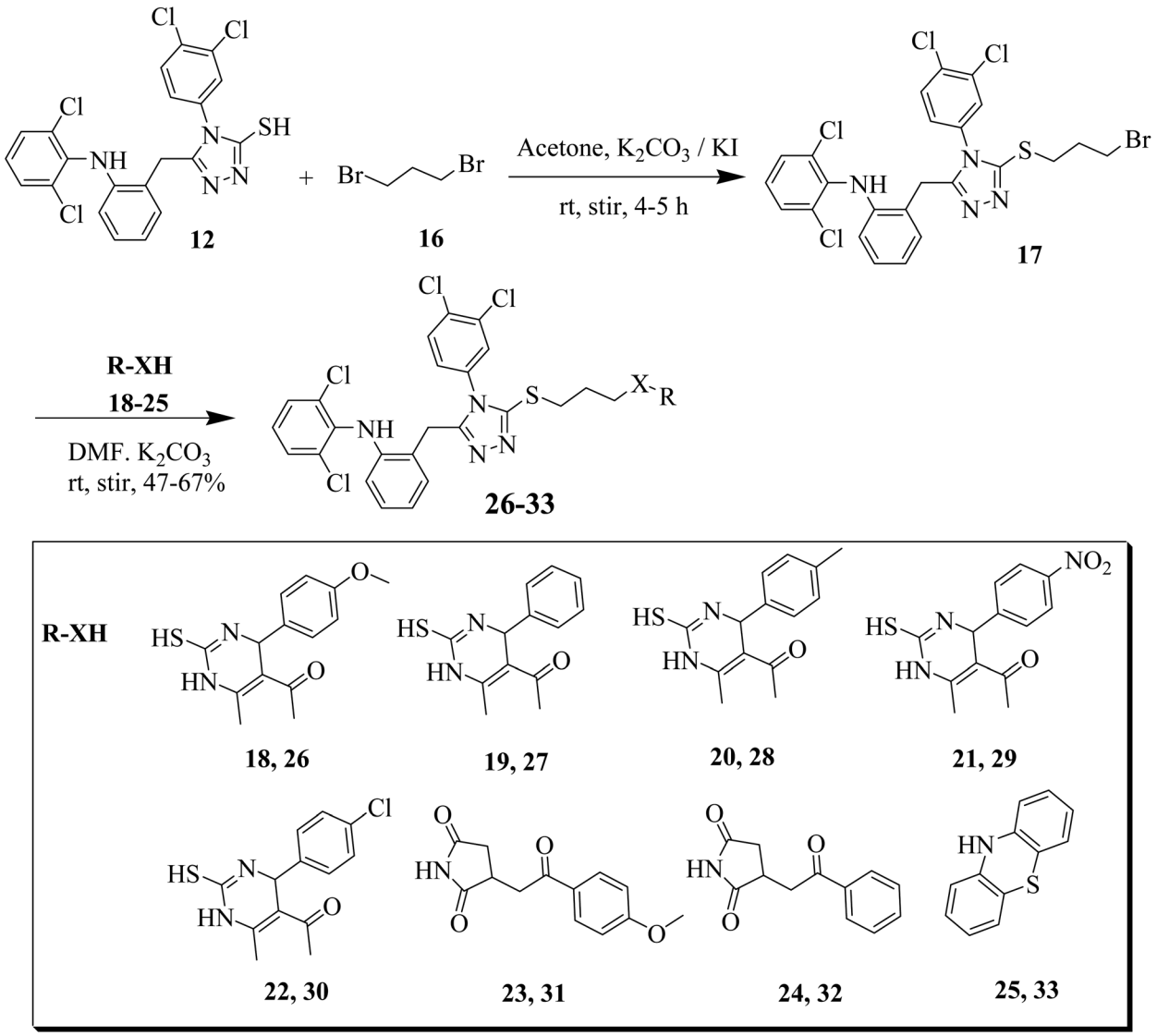

Scheme 3 Synthesis of derivatives of **26–33**.

concentration. This showed that COX-2 binding pocket can accommodate only compounds with less bulky substituents. Compared with lead compound **12**, pyrazoline-sulfonamide derivative **39** was able to show a comparable COX-2 inhibition profile (IC_{50} = 0.60 μM). However, compound **39** showed good 5-LOX inhibition with IC_{50} value of 0.98 μM.

The Ellman method was used to assess the inhibitory potential of synthesized derivatives against eeAChE and eqBChE. Structural modification on diclofenac derivative **12** further increases eeAChE/eqBChE activity. Intermediate thiosemicarbazide **11** emerged as improved and selective eeAChE inhibitor compared with lead derivative **12**. Excellent inhibition and selectivity results towards eeAChE were obtained by increasing the linker length and with bulky scaffolds. Pyrimidine derivatives **28–30** inhibited eeAChE with a nanomolar concentration of 0.10 μM (100 nM) and 0.09 μM (90 nM) and 0.06 μM (60 nM) respectively. The selectivity index for these compounds were 360, 354 and 159.3 respectively. Pyrrolidine derivative **31** with IC_{50} value of 0.08 μM for eeAChE and 48.10 μM for eqBChE showed highest selectivity of 601.2 toward eeAChE. While phenothiazine derivative **33** showed the best eeAChE inhibitory capacity with IC_{50} value of 0.05 μM (Table 2). The data in Table 2 showed the enhancement of inhibitory potentials of modified derivatives of triazole **12**. However, pyrazoline derivative **39** synthesized from modification of starting diclofenac **7** emerged as most potent eeAChE inhibitor with IC_{50} value of 0.03 μM. Pyrazoline derivative **39** was also found most potent towards eqBChE with IC_{50} of 0.91 μM.

All the synthesized compounds were also assessed for their MAO-A and MAO-B inhibitory activity. Structural analysis of MAO-B showed that the binding pocket is a bipartite (two subpockets) elongated hydrophobic cavity divided by Ile199. *In vitro* enzyme inhibition results presented in Table 2 showed that thiosemicarbazide (**11**) and pyrrolidine derivatives **31** and **32**, phenothiazine analog **33** and pyrazoline derivative **39** inhibit MAO-B in nanomolar concentration. We believe that high

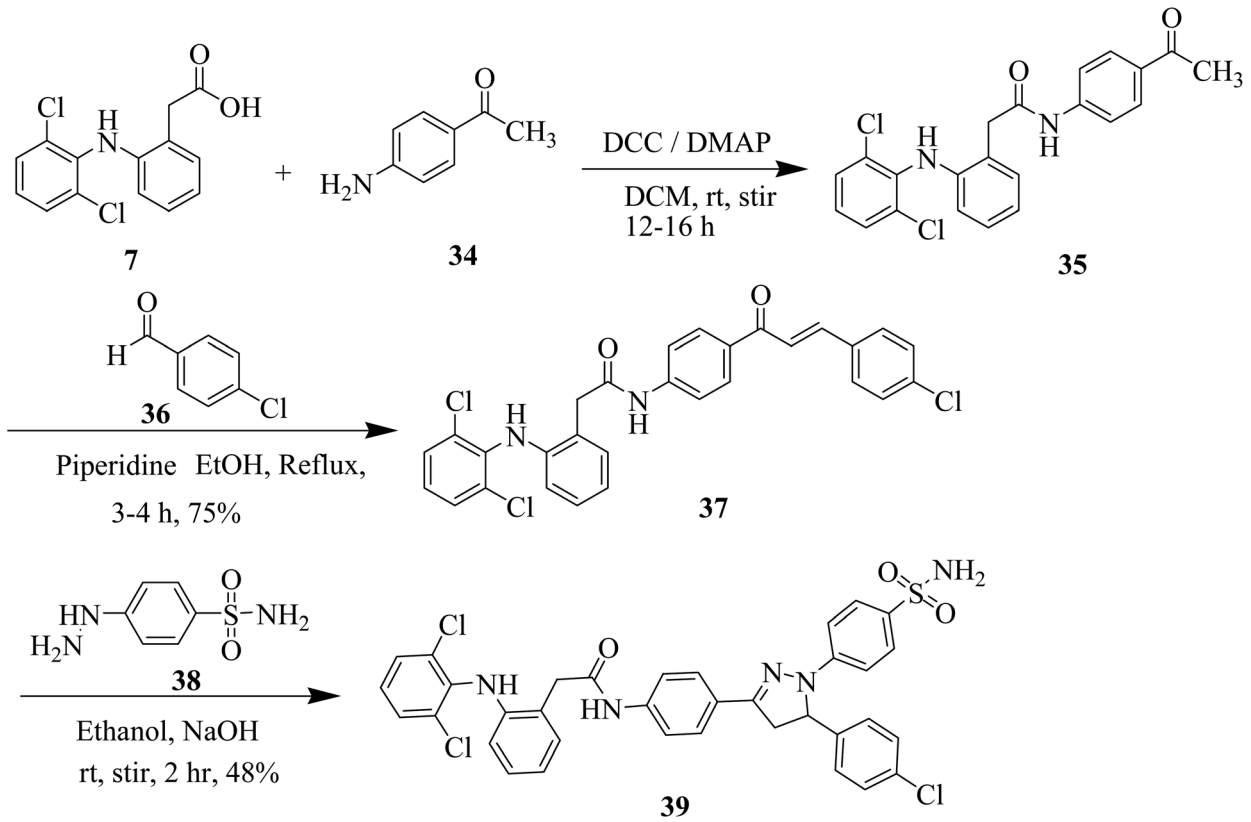

Scheme 4 Synthesis of pyrazoline derivative of diclofenac **39**.

Table 1 COX-2 and 5-LOX inhibition results of the synthesized compounds

	IC_{50} (μM) ± SEM	
Comp.	COX-2	5-LOX
11	1.29 ± 0.11	11.38 ± 1.03
12	0.69 ± 0.13	75.51 ± 1.57
15	0.16 ± 0.04	3.42 ± 0.21
26	NA[a]	35.03 ± 1.71
27	NA	29.81 ± 1.03
28	NA	21.64 ± 1.19
29	NA	14.21 ± 1.08
30	NA	39.54 ± 1.55
31	NA	51.29 ± 1.37
32	NA	48.33 ± 1.42
33	23.01 ± 0.92	9.11 ± 0.08
39	0.60 ± 0.03	0.98 ± 0.01
Diclofenac	4.80 ± 0.11	—
Celecoxib	0.05 ± 0.01	—
Zileuton		0.65 ± 0.04

[a] NA = no activity found in tested concentration.

activity of these compounds is due to their linear conformation like safinamide (docking section) into the elongated binding site of MAO-B. Compound **31** with IC_{50} value of 4.63 μM and 0.024 μM toward MAO-A and MAO-B respectively showed excellent selectivity index of 193. Pyrazoline derivative **39** emerged as most potent MAO-B inhibitor with IC_{50} value of 0.01 μM. However, **39** also inhibited MAO-A in low submicromolar concentration. The selectivity index calculated for **39** is 61.

Good inhibition of MAO-A by dihydropyrimidine derivatives **26–29** is supposed to be due to its curved binding site. Reference drug safinamide is 265 times more potent toward MAO-B compared with MAO-A.

2.4 Toxicity studies

Before submitting the samples for animal studies (*in vivo* toxicity studies), first of all we predicted the toxicity profile of the selected compounds by using online AdmetSAR software. We found toxicity profiles in Category III. Then we proceeded for in vitro neurotoxicity assay.

2.4.1 Neurotoxicity assay. MTT was used on neuroblastoma SH-SY5Y cells to assess the neurotoxic effect of our synthesized compounds, as previously described.[5,29,30] The viability of cells was evaluated at concentrations of 1, 10, 20, 40 and 80 μM with corresponding positive control donepezil. Most active AChE inhibitors **15**, **30**, **33** and **39** were selected for this assay. Fig. 2 sums up the results. The results showed that compounds **30–39** showed no neurotoxicity at studied concentrations after incubation for 48 hours. However, at higher concentration (80 μM) compound **15** displayed some effects on SHSY5Y cell viability. Hence, compound **15** showed low neurotoxicity to SHSY5Y cells at high tested concentration.

Table 2 Cholinesterase and human monoamine oxidase inhibition results of the synthesized compounds

	IC_{50} (μM) ± SEM			IC_{50} (μM) ± SEM		
Comp.	eeAChE	eqBChE	SI (IC_{50} eqBChE/IC_{50} eeAChE)	hMAO-A	hMAO-B	SI (IC_{50} hMAO-A/IC_{50} hMAO-B)
11	0.79 ± 0.08	29.55 ± 1.04	37.4	20.28 ± 0.11	0.081 ± 0.009	250.4
12	2.58 ± 0.41	56.39 ± 1.28	21.8	11.28 ± 1.01	13.07 ± 1.22	0.8
15	0.11 ± 0.01	2.99 ± 0.33	27.2	1.21 ± 0.07	0.89 ± 0.33	1.3
26	0.53 ± 0.01	0.94 ± 0.11	1.8	2.36 ± 0.73	8.28 ± 0.01	0.3
27	0.47 ± 0.02	11.22 ± 0.98	23.9	1.44 ± 0.04	10.08 ± 0.07	0.1
28	0.10 ± 0.07	36.01 ± 1.31	360.1	2.39 ± 0.21	15.21 ± 0.01	0.1
29	0.09 ± 0.01	31.89 ± 1.33	354.3	1.26 ± 0.09	9.13 ± 0.03	0.1
30	0.06 ± 0.01	9.55 ± 1.01	159.1	0.91 ± 0.03	1.32 ± 0.01	0.7
31	0.08 ± 0.01	48.10 ± 1.51	601.2	4.63 ± 0.31	0.024 ± 0.001	193
32	0.39 ± 0.08	3.39 ± 0.83	8.7	6.48 ± 0.39	0.106 ± 0.004	61.1
33	0.05 ± 0.00	5.89 ± 1.00	117.8	8.55 ± 0.26	0.13 ± 0.01	65.7
39	0.03 ± 0.01	0.91 ± 0.16	30.33	0.61 ± 0.08	0.010 ± 0.001	61
Donepezil	0.05 ± 0.01	5.4 ± 0.27	108.0	—	—	—
Safinamide	—	—	—	6.75 ± 0.44	0.025 ± 0.003	270

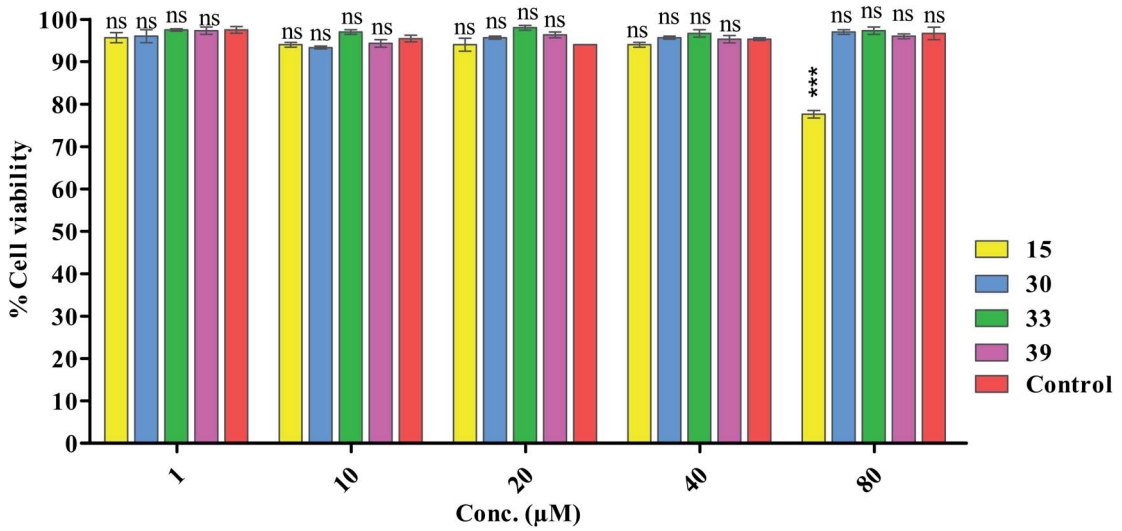

Fig. 2 The MTT assay was used to determine the cell viability of the tested compounds at varied doses in the neuroblastoma SH-SY5Y cell line. The Bonferroni test was used after the two-way ANOVA. *$P = 0.05$, **$P = 0.01$, ***$P = 0.001$, ns; non-significant when compared to the control group; $n = 3$, *$P = 0.05$, **$P = 0.01$, ***$P = 0.001$, ns; non-significant when compared to the control group.

2.4.2 Acute toxicity. For subsequent acute toxicity studies, we selected 4 most active compounds (**15**, **31**, **33**, and **39**) from each series as representative compounds. Table 3 summarizes the key findings. Each group of animals received doses ranging from 50 to 2000 mg kg^{-1} body weight. There were no clinical signs in the central nervous system, mucous membranes, fur, skin, or autonomic nervous system, and all animals were found alive. Furthermore, in the tested doses, no evidence of tremors/convulsions, lethargy, or any abnormal behavior were observed in the examined animals. A dose of 300–2000 mg kg^{-1} is deemed safe and harmless in the case of acute oral toxicity.

Table 3 Specification of the animal grouping and drug quantity given for the acute toxicity studies with various compounds

No. of groups	Animals	Tested synthesized compounds (**15**, **30**, **33** and **39**)
1	8	50
2	8	100
3	8	200
4	8	300
5	8	400
6	8	500
7	8	1000
8	8	2000

2.5 PAMPA BBB assay

The penetration of the blood–brain barrier (BBB) is a crucial concern in the development of Alzheimer's disease (AD)

Table 4 The PAMPA-BBB permeability (Pe) values for the standard drug donepezil, potent compounds, and commercial drugs with the prediction of their BBB penetration

Compounds label	Permeability (PAMPA-BBB)[a] $Pe_{(tested)}$ (10^{-6} cm s^{-1})	Prediction (PAMPA-BBB) (CNS+[b], CNS−[c])
Evaluation of Pe (10^{-6} cm s^{-1}) for the test compounds and standard		
15	6.36 ± 0.30	CNS+
30	8.21 ± 0.15	CNS+
33	9.05 ± 0.20	CNS+
39	7.55 ± 0.14	CNS+
Donepezil	6.55 ± 0.10	CNS+
Validation of the model by seven commercial drugs		
Diazepam	15.30 ± 0.12	CNS+
Atenolol	0.75 ± 0.10	CNS−
Alprazolam	5.60 ± 0.21	CNS+
Lomefloxacin	1.12 ± 0.09	CNS−

[a] Data represent are the assay mean for the marketed drugs ($n = 3$). [b] 'CNS+' (prediction of high BBB permeation); Pe (10^{-6} cm s^{-1}) > 4.39. [c] 'CNS−' (prediction of low BBB permeation); Pe (10^{-6} cm s^{-1}) < 1.78.

therapies. Using previously reported procedure, we performed a parallel artificial membrane permeation assay (PAMPA).[26,31,32] We selected all the four compounds *i.e.* **15**, **30**, **33** and **39** for this purpose. All the selected compounds concomitantly inhibited the tested enzymes in nanomolar range. Table 4 summarizes the results of the PAMPA BBB penetration, and all the tested compounds were found to be BBB penetrant. The existence of hydrophobic functional groups could explain these observations.

2.4 Molecular docking studies

To explore binding interaction of synthesized compounds with the active site of target enzymes, docking experiments were performed. All the synthesized compounds were docked into the active sites of AChE, BChE, MAO-A, MAO-B, COX-2 and 5-LOX with accession code 1EVE, 4BDS, 2Z5V, 2V5Z, 1CX2 and 6N2W. We assessed docking reliability by re-docking native ligands prior to predicting the docking poses of synthesized compounds. The measured RMSD values were within acceptable ranges (<2.0 Å).

Dual binding site inhibitors of AChE interact with the catalytic active site (CAS) and peripheral anionic site (PAS). Trp84, Tyr130, Phe330 and Phe331 are important amino acid residues present in CAS. While Tyr70, Asp72, Tyr121, Trp279 and Tyr334 are important residues in PAS. Ser200, Glu327, His440 are present in catalytic triads, Phe288 and Phe290 in acyl pocket and Gly118, Gly119 and Ala201 in oxyanion hole of AChE. Compound **33** ($IC_{50} = 0.05$ μM) is supposed to inhibit AChE by interacting with active site *via* formation of six hydrophobic interactions (π–π and π–sulfur type) and one halogen interaction between chlorine atom and Tyr334 (Fig. 3a). Potent compound **39** showed bifurcated π–π, H-bond and π–sulfur interactions with important residues present in CAS (Trp84, Phe330, Phe331) and PAS (Tyr121, Trp279, Tyr334) of AChE (Fig. 3b).

MAO-B binding pocket is a bipartite (two sub-pockets) elongated hydrophobic cavity divided by Ile199. The entrance cavity contains Pro102, Pro104, Trp119, Leu164, Ile198, Ile199, Thr201, Ile316, and Tyr326. While substrate cavity is formed by Ser59, Tyr60, Cys172, Gln206, Tyr398 and Tyr435.[33,34]

In vitro MAO-B inhibition results (Table 2) demonstrated that the high inhibition potentials of thiosemicarbazide analog **11** and pyrrolidine derivatives **31** and **32** may be due to their linear conformation like safinamide (docking section) into the elongated binding site of MAO-B. The three-dimensional (3D) overlaid diagrams of **11** and **31** and reference drug safinamide are shown in Fig. 4a and b. Two-dimensional (2D) interaction

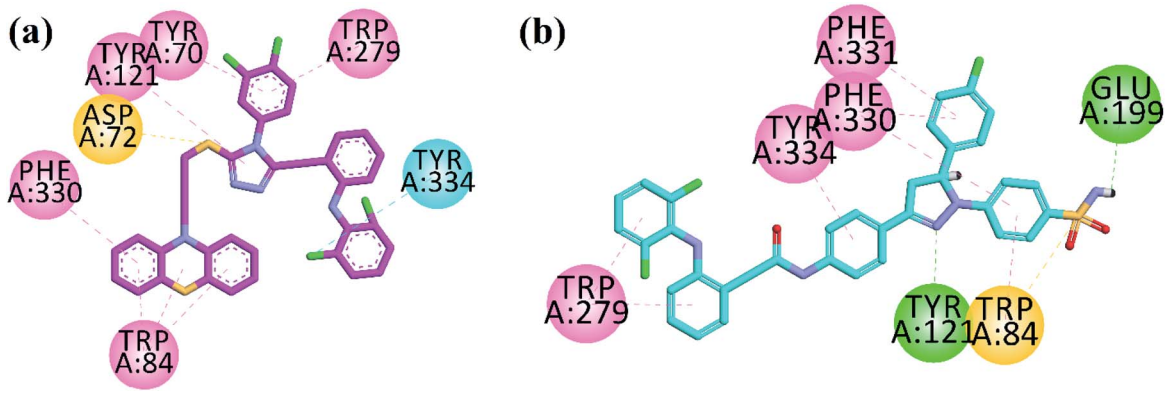

Fig. 3 2D interaction plot of synthesized compounds **33** (a) and **39** (b) in the active site of AChE.

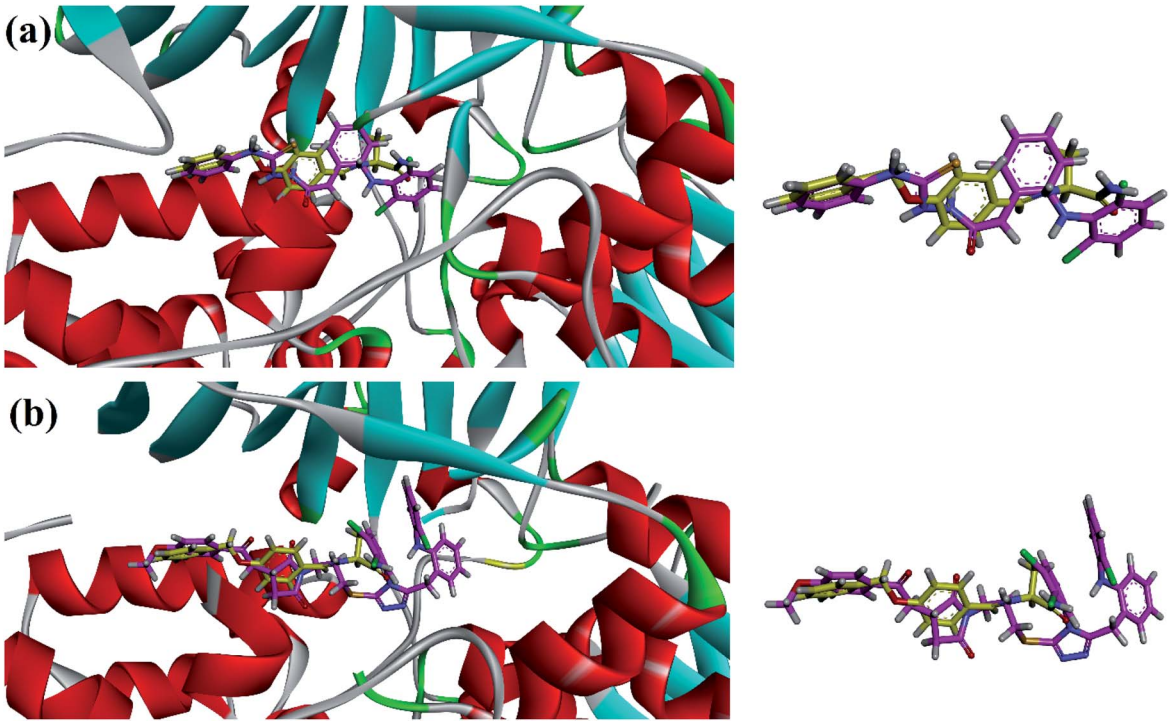

Fig. 4 3-D superposed diagram of compound **11** (a), **31** (b) and reference drug safinamide (yellow sticks) into the binding site of MAO-B.

plots shown in Fig. 5 revealed that the ligand (**11**)–enzyme complex is stabilized by forming hydrogen bonds, π–π and π–sulfur, interactions. The entrance cavity residues (Ile199/Tyr326) and substrate cavity residues Tyr60, Cys172, Gln206, Tyr398 and Tyr435 are involved in these types of interactions (Fig. 5a). While residues Tyr188, Ile199, Tyr60, Cys172, Gly205, Gln206, Tyr398 and Tyr435 are involved in stabilizing ligand (**31**)–enzyme complex (Fig. 5b).

Superposed binding poses of most active MAO-B pyrazoline analog **39** over safinamide demonstrated that pyrazoline core oriented toward entrance cavity while diclofenac part toward substrate cavity (Fig. 6a). Very high inhibition potential may be due six hydrogen bond interactions with Arg42, Cys197, Ile19, 9Gln206, Tyr326 and Trp388 (Fig. 6b).

3 Experimental

3.1 General

All reagents and solvents were purchased from Sigma Aldrich and were used without any purification. Diclofenac acid was purchased from Alfa Aesar. ^{1}H NMR and ^{13}C NMR spectra were recorded in deuterated solvent on Bruker 400 MHz spectrometers, with TMS as an internal reference. Melting points were determined in open capillary using Stuart melting point apparatus (SMP10). TLC plates pre-coated with silica gel 60F254 were used to monitor the progress of all reactions. The synthesized compounds that were more than 95% pure by HPLC (Schimadzu) were submitted for biological evaluation. MeOH/Water (1% CH_3COONH_4, w/v) was used as isocratic solvent system in the 70 : 30 ration with a flow rate of 1.0 mL min^{-1}.

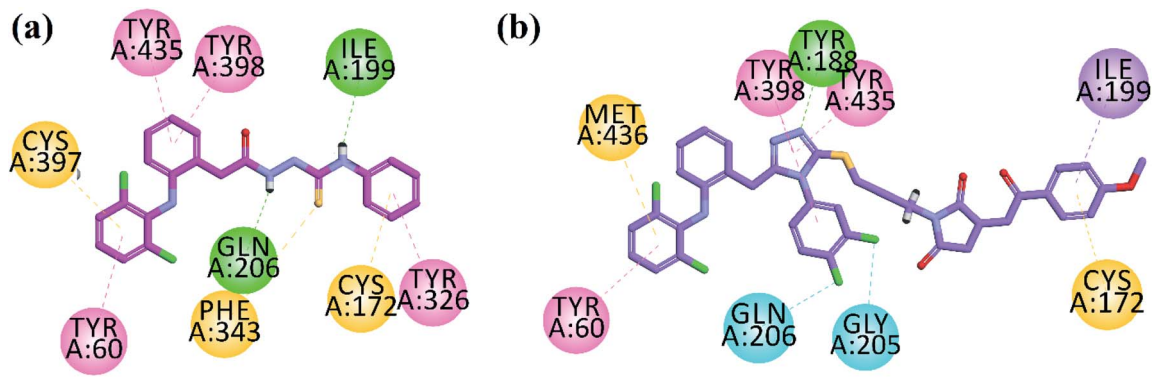

Fig. 5 2D interaction plots of synthesized compound **11** (a) and **31** (b) in the active site of MAO-B (PDB ID = 2V5Z).

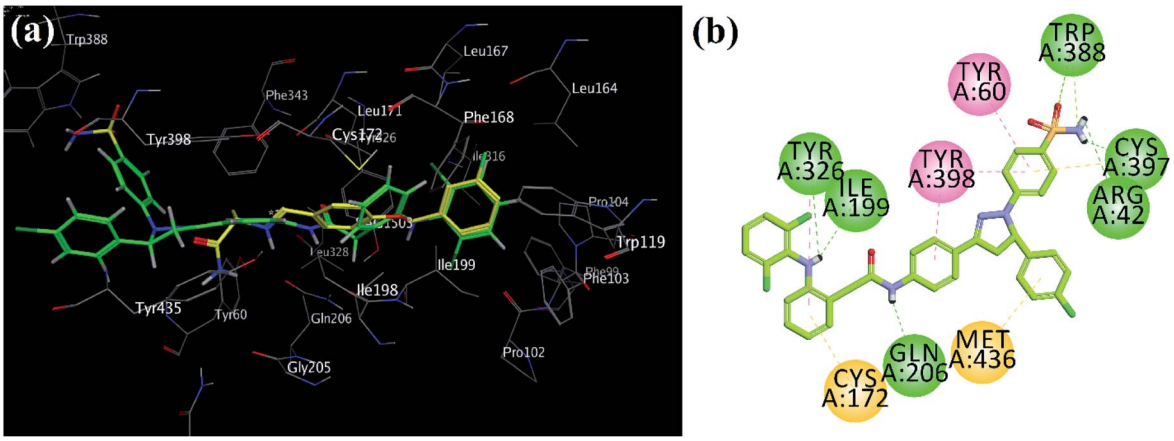

Fig. 6 (a) MOE generated 3D superpose diagram of compound **39** (green) and reference drug safinamide (yellow sticks) into the binding site of MAO-B; (b) 2D interaction plots of synthesized compound **39** in the active site of MAO-B (PDB ID = 2V5Z).

3.2 General method for the synthesis of diclofenac methyl ester (8)

Diclofenac acid **7** (20 mmol) was stirred at 0 °C in dry acetone followed by addition of 1.5 equivalent of thionyl chloride. Reaction mixture was stirred initially for two hours at 0 °C and then 1 hour at an ambient temperature then refluxed for three hours to yield acid chloride (**8**).

White crystalline solid; R_f = 0.69 (*n*-hexane : ethyl acetate 4 : 1); yield 86%; mp 98–99 °C. ^{1}H NMR (400 MHz, DMSO-d6) δ 7.44 (d, J = 8.1 Hz, 2H, Ar–H), 7.25 (dd, J = 7.4, 2.4 Hz, 1H, Ar–H), 7.08 (t, J = 8.1 Hz, 1H, Ar–H), 6.98 (td, J = 7.7, 3.8 Hz, 1H, Ar–H), 6.94 (s, 1H, NH), 6.76 (t, J = 7.5 Hz, 1H, Ar–H), 6.22 (d, J = 7.8 Hz, 1H, Ar–H), 3.86 (s, 2H, CH_2). ^{13}C NMR (100 MHz, DMSO-d6) δ 172.41, 145.05, 143.37, 130.89, 130.61, 129.44, 127.30, 125.46, 123.93, 119.26, 116.29, 52.20, 37.93.

3.3 General method for the synthesis of diclofenac hydrazide (9)

A mixture of diclofenac acid chloride (8, 30 mmol) and hydrazine hydrate (50 mmol) was refluxed in absolute ethanol (30 mL) for 6–7 h. Completion of reaction was monitored through TLC, the solid product was collected through filtration, dried and recrystallized from ethanol.

White amorphous solid; R_f = 0.16 (*n*-hexane : ethyl acetate 4 : 1); yield 84% mp 134–136 °C. ^{1}H NMR (400 MHz, DMSO-d6) δ 9.09 (s, 1H, NH), 7.44 (d, J = 8.1 Hz, 2H, Ar–H), 7.19–7.09 (m, 2H, Ar–H), 6.98 (t, J = 7.6 Hz, 1H, Ar–H), 6.94 (s, 1H, NH), 6.79 (t, J = 7.5 Hz, 1H, Ar–H), 6.22 (d, J = 7.8 Hz, 1H, Ar–H), 4.28 (s, 2H, NH_2), 3.44 (s, 2H, CH_2). ^{13}C NMR (100 MHz, DMSO-d6) δ 171.2, 143.6, 143.3, 130.6, 129.4, 129.1, 127.8, 125.4, 123.9, 123.2, 116.9, 38.39.

3.4 General method for the synthesis of thiosemicarbazide (11)

An equimolar mixture of diclofenac hydrazide (20 mmol) and aryl isothiocyanate (10, 20 mmol) was refluxed in dry acetone for 5–6 h. After completion of reaction, the reaction mixture was cooled, solid product was thus separated out, dried and was recrystallized from ethanol.

White solid; R_f = 0.46 (*n*-hexane : ethyl acetate 4 : 1); yield 81%; mp 195–197 °C. ^{1}H NMR (400 MHz, DMSO-d6) δ 10.52 (br s, 1H, NH), 9.97 (br s, 1H, NH), 9.51 (br s, 1H, NH), 7.97 (br s, 1H, NH), 7.81 (s, 1H, Ar–H), 7.60 (d, J = 8.7 Hz, 1H, Ar–H), 7.53 (d, J = 8.1 Hz, 2H, Ar–H), 7.40 (d, J = 9.0 Hz, 1H, Ar–H), 7.25 (d, J = 7.1 Hz, 1H, Ar–H), 7.18 (t, J = 8.1 Hz, 1H, Ar–H), 7.07 (t, J = 7.1 Hz, 1H, Ar–H), 6.88 (t, J = 7.2 Hz, 1H, Ar–H), 6.31 (d, J = 7.9 Hz, 1H, Ar–H), 3.70 (s, 2H, CH_2). ^{13}C NMR (100 MHz, DMSO-d6) δ 181.9, 169.8, 143.6, 143.4, 140.1, 131.8, 130.6, 129.4, 129.1, 128.9, 127.8, 125.5, 124.8, 124.0, 123.9, 123.3, 118.8, 116.9, 38.2. HRMS (EI) calcd for $C_{21}H_{16}Cl_4N_4OS$ [M^+]: 511.9799 found 511.9783.

3.5 General method for the synthesis of 5-(2-(2,6-dichlorophenylamino)benzyl)-4-(3,4 dichlorophenyl)-4*H*-1,2,4-triazole-3-thiol (12)

Thiosemicarbazide **11** (15 mmol) was added dropwise to the stirred solution of NaOH (5%, 30 mL). The reaction mixture was allowed to reflux for 3–4 h. After cooling, the reaction mixture was filtered, and the filtrate was acidified with 6 N HCl to pH 2–3. The precipitated solid was filtered, washed thoroughly with water and recrystallized with ethanol.

Peach solid; R_f = 0.59 (*n*-hexane : ethyl acetate 4 : 1); yield 79%; mp 254–256 °C. ^{1}H NMR (500 MHz, DMSO-d6) δ 13.89 (s, 1H, SH), 8.13 (s, 1H, NH), 7.79 (d, J = 9.1 Hz, 1H, Ar–H), 7.71 (d, J = 2.3 Hz, 1H, Ar–H), 7.51 (d, J = 8.0 Hz, 2H, Ar–H), 7.40 (dd, J = 8.5, 2.4 Hz, 1H, Ar–H), 7.21 (t, J = 8.0 Hz, 1H, Ar–H), 7.01 (td, J = 9.0, 1.2, Hz, 1H, Ar–H), 6.86 (dd, J = 8.6, 1.3 Hz, 1H, Ar–H), 6.73 (td, J = 7.5, 1.0 Hz, 1H, Ar–H), 6.14 (d, J = 8.0 Hz, 1H, Ar–H), 3.97 (s, 2H, CH_2). ^{13}C NMR (125 MHz, DMSO-d6) δ; 168.4, 150.8, 143.3, 137.5, 133.9, (132.9)2, 132.0, 131.8, 131.6, 131.1, (129.5)3, 128.3, (126.8)2, 123.1, 120.6, 115.9, 28.6. HRMS (EI) calcd for $C_{21}H_{14}Cl_4N_4S$ [M^+]: 493.9693 found 493.9679.

3.6 General method for the synthesis of 4-((5-(2-(2,6-dichlorophenylamino)benzyl)-4-(3,4-dichlorophenyl)-4*H*-1,2,4-triazol-3-ylthio)methylamino)benzenesulfonamide (15)

At 0 °C, sulfanilamide (**14**) was stirred for 30 minutes in methanol in the presence of 5 mmol formalin (7, 1 equiv.). Compound **12** in methanol was then added and the reaction

mixture was refluxed for three hours after some time. Using thin layer chromatography, reaction progress was noted. After the completion of reaction, the reaction mixture was kept in the refrigerator overnight. The formed product was filtered, washed, and recrystallized using ethanol.

Off-white solid; R_f = 0.52 (DCM : MeOH 10 : 1); yield 56%; ^{1}H NMR (400 MHz, DMSO-d6, ppm) δ: 9.80 (brs, 1H, NH), 7.92 (d, 1H, J = 8 Hz, ArH), 7.81 (d, 2H, J = 8 Hz, ArH), 7.69 (brs, 1H, NH), 7.50–7.46 (m, 4H, ArH), 7.43–7.39 (m, 2H, ArH), 7.31–7.26 (m, 3H, ArH), 7.21–7.19 (m, 2H, ArH), 5.95 (brs, 2H, NH_2), 4.86 (s, 2H, CH_2), 3.97 (s, 2H, CH_2); ^{13}C NMR (100 MHz, DMSO-d6), δ. 166, 150.2, 144.3, 138.6, 136.3, 134.6, (133.4)2, 130.7, 130.0, (129.7)3, 128.9, (127.8)3, (126.9)2, 126.0, 125.7, 122.1, 120.4, 119.2, (112.7)2, 57.4, 21.5. LC-MS: m/z = 681.4 $[M + H]^+$; analysis calculated for $C_{28}H_{22}Cl_4N_6O_2S_2$. C, 49.42; H, 3.26; Cl, 20.84; N, 12.35; O, 4.70; S, 9.42. Observed; C, 49.49; H, 3.24; N, 12.32.

3.7 General method for the synthesis of intermediate 17

Diclofenac intermediate **12** (20 mmol) and 1,3 dibromopropane **16** were stirred in the presence of K_2CO_3/KI in acetone, the mono bromo diclofenac triazole intermediate **17** was obtained. On completion of reaction, the residue left after evaporation of solvent was dissolved in $NaHCO_3$ solution and extraction was carried out with ethyl acetate (4 × 30 mL) followed by washing the combined extract with brine (2 × 20 mL) then dried over anhydrous Na_2SO_4. Solvent was removed under reduced pressure. The compound **17** obtained was used without further purification in next step.

3.7.1 *N*-(2-((5-(3-Bromopropylthio)-4-(3,4-dichlorophenyl)-4*H*-1,2,4-triazol-3-yl)methyl) phenyl)-2,6-dichlorobenzenamine (17). Yield 74%; ^{1}H NMR (400 MHz, DMSO-d6, ppm) δ: 8.11 (s, 1H, NH), 7.73 (d, J = 9.1 Hz, 1H, Ar–H), 7.69 (d, J = 2.3 Hz, 1H, Ar–H), 7.47 (d, J = 8.0 Hz, 2H, Ar–H), 7.37 (dd, J = 8.5, 2.4 Hz, 1H, Ar–H), 7.22 (t, J = 8.0 Hz, 1H, Ar–H), 7.03 (td, J = 9.0, 1.2, Hz, 1H, Ar–H), 6.83 (dd, J = 8.6, 1.3 Hz, 1H, Ar–H), 6.71 (td, J = 7.5, 1.0 Hz, 1H, Ar–H), 6.12 (d, J = 8.0 Hz, 1H, Ar–H), 3.93 (s, 2H, CH_2), 3.35 (t, 2H, CH_2), 2.97 (t, 2H, CH_2), 2.24 (m, 2H, CH_2). ^{13}C NMR (100 MHz, DMSO-d6) δ: 169.2, 151.3, 144.2, 136.9, (133.3)2, 131.9, 131.1, 130.5, 129.9, 129.2, (128.8)3, 127.7, (126.9)2, 124.4, 121.2, 116.6, 36.8, 36.6, 31.8, 24.6. LC-MS: m/z = 618.21 $[M + H]^+$; analysis calculated for $C_{24}H_{19}BrCl_4N_4S$; C, 46.70; H, 3.10; N, 9.08. Observed: C, 46.76; H, 3.08; N, 9.05.

3.8 General method for the synthesis of compounds 26–33

A solution of monobromo intermediate **17** (5 mmol), R-XH (18–25, 10 mmol) and K_2CO_3 in DMF were stirred for 3 h. After completion of reaction, the mixture was poured into water and extracted with ethyl acetate (4 × 20 mL), washed with water then brine and dried over anhydrous $MgSO_4$, filtered and concentrated under reduced pressure. The crude products (**26–33**) were purified by using silica gel chromatography (DCM/MeOH; 10 : 1).

3.8.1 1-(2-(3-(5-(2-(2,6-Dichlorophenylamino)benzyl)-4-(3,4-dichlorophenyl)-4*H*-1,2,4-triazol-3-ylthio)propylthio)-4-(4-methoxyphenyl)-6-methyl-1,4-dihydropyrimidin-5-yl)ethenone (26). White solid; R_f = 0.46 (DCM/MeOH 10 : 1); yield 61%; mp 195–197 °C. HPLC purity = 97.9% (C18 RP, acetonitrile/H_2O 97 : 3), TR = 13.7 min. ^{1}H NMR (400 MHz, DMSO-d6, ppm) δ: 9.73 (brs, 1H, NH), 8.32 (brs, 1H, NH), 7.89 (d, 1H, ArH), 7.62 (s, 1H, ArH), 7.43 (d, 1H, ArH), 6.98 (d, 2H, ArH), 6.85 (d, 2H, ArH), 6.65 (t, 1H, ArH), 6.61 (d, 2H, ArH), 6.57 (m, 4H, ArH), 5.17 (s, 1H, CH), 4.04 (s, 2H, CH_2), 3.83 (s, 3H, OCH_3), 2.95 (t, 2H, CH_2), 2.85 (t, 2H, CH_2), 2.43 (m, 2H, CH_2), 2.31 (s, 3H, CH_3), 2.35 (s, 3H, CH_3). ^{13}C NMR (100 MHz, DMSO-d6), δ. 1.97.1, 164.3, 161.6, 158.8, 155.2, 146.5, 137.7, 135.3, 134.7, (132.2)2, 131.4, (130.9)2, 130.1, (129.8)3, 128.8, 128.1, (127.2)2, 126.9, 126.2, 120.4, 119.5, 118.3, (114.4)2, 111.5, 55.5, 51.3, 36.3, 29.3, 27.7, 25.4, 21.1, 15.6. LC-MS: m/z = 813.6 $[M + H]^+$; analysis calculated for $C_{38}H_{34}Cl_4N_6O_2S_2$. C, 56.16; H, 4.22; Cl, 17.45; N, 10.34; O, 3.94; S, 7.89. Observed; C, 56.21; H, 4.21; N, 10.31.

3.8.2 4-(2-(3-(5-(2-(2,6-Dichlorophenylamino)benzyl)-4-(3,4-dichlorophenyl)-4*H*-1,2,4-triazol-3-ylthio)propylthio)-6-methyl-4-phenyl-1,4-dihydropyrimidin-5-yl)ethenone (27). White solid; R_f = 0.43 (DCM/MeOH 10 : 1); yield 63%; mp 189–195 °C. HPLC purity = 96.3% (C18 RP, acetonitrile/H_2O 97 : 3), TR = 7.1 min. ^{1}H NMR (400 MHz, DMSO-d6, ppm) δ: 9.69 (brs, 1H, NH), 8.28 (brs, 1H, NH), 7.86 (d, 1H, ArH), 7.61 (s, 1H, ArH), 7.45 (d, 1H, ArH), 7.04 (m, 5H, ArH), 6.95 (d, 2H, ArH), 6.63 (t, 1H, ArH), 6.58 (m, 4H, ArH), 5.19 (s, 1H, CH), 4.02 (s, 2H, CH_2), 2.93 (t, 2H, CH_2), 2.86 (t, 2H, CH_2), 2.44 (m, 2H, CH_2), 2.33 (s, 3H, CH_3), 2.37 (s, 3H, CH_3). ^{13}C NMR (100 MHz, DMSO-d6), δ. 195.3, 164.7, 162.5, 158.2, 155.5, 146.6, 137.3, 136.3, 135.5, (132.4)2, 130.7, (129.5)2, (128.8)2, (128.1)3, (127.3)2, 126.2, 125.3, 121.3, 120.5, 117.9, 115.5, 112.3, 52.5, 37.3, 29.6, 27.2, 25.1, 21.5, 15.1. LC-MS: m/z = 783.63 $[M + H]^+$; analysis calculated for $C_{37}H_{32}Cl_4N_6OS_2$. C, 56.78; H, 4.12; Cl, 18.12; N, 10.74; O, 2.04; S, 8.19. Observed; C, 56.84; H, 4.10; N, 10.71.

3.8.3 1-(2-(3-(5-(2-(2,6-Dichlorophenylamino)benzyl)-4-(3,4-dichlorophenyl)-4*H*-1,2,4-triazol-3-ylthio)propylthio)-6-methyl-4-*p*-tolyl-1,4-dihydropyrimidin-5-yl)ethenone (28). Off white solid; R_f = 0.47 (DCM/MeOH 10 : 1); yield 59%; mp 183–189 °C. HPLC purity = 97.7% (C18 RP, acetonitrile/H_2O 97 : 3), TR = 13.2 min. ^{1}H NMR (400 MHz, DMSO-d6, ppm) δ: 9.69 (brs, 1H, NH), 8.30 (brs, 1H, NH), 7.88 (d, 1H, ArH), 7.60 (s, 1H, ArH), 7.41 (d, 1H, ArH), 6.94 (d, 2H, ArH), 6.82 (d, 2H, ArH), 6.67 (t, 1H, ArH), 6.63 (d, 2H, ArH), 6.56 (m, 4H, ArH), 5.18 (s, 1H, CH), 4.01 (s, 2H, CH_2), 2.94 (t, 2H, CH_2), 2.83 (t, 2H, CH_2), 2.44 (m, 2H, CH_2), 2.37 (s, 3H, CH_3), 2.32 (s, 3H, CH_3), 2.34 (s, 3H, CH_3). ^{13}C NMR (100 MHz, DMSO-d6), δ. 197.3, 164.7, 162.5, 158.2, 155.5, 146.6, 137.3, 136.3, (135.5)2, (132.4)2, 131.7, 130.7, (129.7)2, (128.8)3, 128.1, (127.3)2, 126.2, 121.3, 120.5, 117.9, 115.5, 112.3, 52.5, 37.3, 29.6, 27.2, 25.1, 21.5, 15.1. LC-MS: m/z = 797.65 $[M + H]^+$; analysis calculated for $C_{38}H_{34}Cl_4N_6OS_2$. C, 57.29; H, 4.30; Cl, 17.80; N, 10.55; O, 2.01; S, 8.05. Observed: C, 57.34; H, 4.28; N, 10.52.

3.8.4 1-(2-(3-(5-(2-(2,6-Dichlorophenylamino)benzyl)-4-(3,4-dichlorophenyl)-4*H*-1,2,4-triazol-3-ylthio)propylthio)-6-methyl-4-(4-nitrophenyl)-1,4-dihydropyrimidin-5-yl)ethenone (29). White solid; R_f = 0.43 (DCM/MeOH 10 : 1); yield 67%; mp 192–198 °C. HPLC purity = 99.2% (C18 RP, acetonitrile/H_2O 98 : 2), TR = 15.5 min. ^{1}H NMR (400 MHz, DMSO-d6, ppm) δ: 9.72 (brs, 1H, NH), 8.33 (brs, 1H, NH), 7.89 (d, 1H, ArH), 7.64 (s, 1H, ArH), 7.43 (d, 1H, ArH), 6.96 (d, 2H, ArH), 6.86 (d, 2H, ArH), 6.68 (t,

1H, ArH), 6.64 (d, 2H, ArH), 6.57 (m, 4H, ArH), 5.19 (s, 1H, CH), 4.05 (s, 2H, CH_2), 2.96 (t, 2H, CH_2), 2.84 (t, 2H, CH_2), 2.46 (m, 2H, CH_2), 2.34 (s, 3H, CH_3), 2.33 (s, 3H, CH_3). ^{13}C NMR (100 MHz, DMSO-d6), δ. 196.6, 165.2, 163.1, 157.2, 155.5, 146.6, 137.5, 136.1, 135.9, (133.4)2, 132.7, 130.2, (129.2)3, 128.8, (128.0)3, (127.8)2, 126.0, 125.6, (122.8)2, 121.5, 118.2, 116.3, 112.3, 55.3, 36.3, 29.1, 27.6, 26.1, 20.5, 16.3. LC-MS: m/z = 828.62 $[M + H]^+$; analysis calculated for $C_{37}H_{31}Cl_4N_7O_3S_2$. C, 53.70; H, 3.78; Cl, 17.13; N, 11.85; O, 5.80; S, 7.75. Observed; C, 53.62; H, 3.80; N, 11.88.

3.8.5 1-(2-(3-(5-(2-(2,6-Dichlorophenylamino)benzyl)-4-(3,4-dichlorophenyl)-4*H*-1,2,4-triazol-3-ylthio)propylthio)-4-(4-chlorophenyl)-6-methyl-1,4-dihydropyrimidin-5-yl)ethenone (30). Off white solid; R_f = 0.49 (DCM/MeOH 10 : 1); yield 65%; mp 190–196 °C. HPLC purity = 99.4% (C18 RP, acetonitrile/H_2O 97 : 3), TR = 11.5 min. ^{1}H NMR (400 MHz, DMSO-d6, ppm) δ: 9.70 (brs, 1H, NH), 8.29 (brs, 1H, NH), 7.85 (d, 1H, ArH), 7.61 (s, 1H, ArH), 7.42 (d, 1H, ArH), 6.91 (d, 2H, ArH), 6.85 (d, 2H, ArH), 6.67 (t, 1H, ArH), 6.63 (d, 2H, ArH), 6.54 (m, 4H, ArH), 5.15 (s, 1H, CH), 4.03 (s, 2H, CH_2), 2.93 (t, 2H, CH_2), 2.80 (t, 2H, CH_2), 2.42 (m, 2H, CH_2), 2.32 (s, 3H, CH_3), 2.30 (s, 3H, CH_3). ^{13}C NMR (100 MHz, DMSO-d6), δ. 1.95.8, 165.5, 163.4, 157.2, 156.4, 146.4, 138.2, 136.8, 135.3, (133.5)2, 132.2, 131.4, (130.9)2, 130.2, (129.6)3, (128.5)2, (127.7)2, 126.5, 125.3, 120.2, 119.4, 118.5, 116.3, 113.1, 51.8, 36.6, 30.6, 27.7, 25.5, 20.3, 15.9. LC-MS: m/z = 817.07 $[M + H]^+$; analysis calculated for $C_{37}H_{31}Cl_5N_6OS_2$. C, 54.39; H, 3.82; Cl, 21.70; N, 10.29; O, 1.96; S, 7.85. Observed; C, 54.33; H, 3.84; N, 10.32.

3.8.6 1-(3-((4-(3,4-Dichlorophenyl)-5-(2-((2,6-dichlorophenyl)amino)benzyl)-4*H*-1,2,4-triazol-3-yl)thio)propyl)-3-(2-(4-methoxyphenyl)-2-oxoethyl)pyrrolidine-2,5-dione (31). White solid; R_f = 0.44 (DCM/MeOH 10 : 1); yield 51%; mp 182–188 °C. HPLC purity = 96.8% (C18 RP, acetonitrile/H_2O 98 : 2), TR = 13.8 min. ^{1}H NMR (400 MHz, DMSO-d6, ppm) δ: 8.18 (brs, 1H, NH), 7.77 (d, 2H, ArH), 7.44 (d, 1H, ArH), 7.61 (s, 1H, ArH), 7.41 (d, 1H, ArH), 6.92 (d, 2H, ArH), 6.85 (d, 2H, ArH), 6.57 (t, 1H, ArH), 6.54 (m, 4H, ArH), 4.03 (s, 2H, CH_2), 3.72 (s, 3H, OCH_3), 3.32 (m, 1H, CH), 3.13 (dd, J = 18.4 Hz, 5.3 Hz, 1H), 2.93 (t, 2H, CH_2), 2.80 (t, 2H, CH_2), 2.73 (dd, J = 18.4 Hz, 9.2, Hz, 1H), 2.42 (m, 2H, CH_2), 2.29 (dd, J = 5.72, 18.2 Hz, 1H), 2.17 (dd, J = 8.2, 18.2 Hz, 1H). ^{13}C NMR (100 MHz, DMSO-d6), δ. 202.2, 176.5, 167.2, 163.5, 139.7, 137.4, 136.2, (133.5)2, 131.1, (130.3)2, (129.7)3, 129.3, 128.9, 128.4, (127.8)2, 127.5, 127.1, 126.7, 126.2, 125.9, 121.3, 119.9, 118.2, (113.3)2, 56.5, 41.2, 38.7, 33.1, 32.6, 26.3, 20.5. LC-MS: m/z = 784.55 $[M + H]^+$; analysis calculated for $C_{37}H_{31}Cl_4N_5O_4S$. C, 56.72; H, 3.99; Cl, 18.10; N, 8.94; O, 8.17; S, 4.09. Observed; C, 56.78; H, 3.97; N, 8.92.

3.8.7 1-(3-((4-(3,4-Dichlorophenyl)-5-(2-((2,6-dichlorophenyl) amino)benzyl)-4*H*-1,2,4-triazol-3-yl)thio)propyl)-3-(2-oxo-2-phenylethyl)pyrrolidine-2,5-dione (32). Off white solid; R_f = 0.46 (DCM/MeOH 10 : 1); yield 47%; mp 195–199 °C. HPLC purity = 99.3% (C18 RP, acetonitrile/H_2O 98 : 2), TR = 13.3 min. ^{1}H NMR (400 MHz, DMSO-d6, ppm) δ: 8.18 (brs, 1H, NH), 7.86 (d, 2H, ArH), 7.44 (d, 1H, ArH), 7.61 (s, 1H, ArH), 7.49 (t, 1H, ArH), 7.41 (d, 1H, ArH), 7.31 (d, 2H, ArH), 6.85 (d, 2H, ArH), 6.57 (t, 1H, ArH), 6.54 (m, 4H, ArH), 4.03 (s, 2H, CH_2), 3.32 (m, 1H, CH), 3.13 (dd, J = 18.4 Hz, 5.3 Hz, 1H), 2.93 (t, 2H, CH_2), 2.80 (t, 2H, CH_2), 2.73 (dd, J = 18.4 Hz, 9.2, Hz, 1H), 2.42 (m, 2H, CH_2), 2.29 (dd, J = 5.72, 18.2 Hz, 1H), 2.17 (dd, J = 8.2, 18.2 Hz, 1H). ^{13}C NMR (100 MHz, DMSO-d6), δ. 201.4, 175.3, 165.9, 162.4, 138.4, 137.3, 135.5, (133.2)2, 130.7, (129.3)2, 129.0, 128.9, 128.6 (128.2)2, (127.9)2, 127.1, 126.9, 126.6, 126.0, 125.3, 120.5, 119.3, 118.8, (113.6)2, 41.6, 36.2, 33.8, 32.3, 25.5, 20.2. LC-MS: m/z = 753.52 $[M + H]^+$; analysis calculated for $C_{36}H_{27}Cl_4N_5O_3S$. C, 57.38; H, 3.88; Cl, 18.82; N, 9.29; O, 6.37; S, 4.26. Observed; C, 57.45; H, 3.86; N, 9.26.

3.8.8 *N*-(2-((5-(4-(4a*H*-Phenothiazin-10(10a*H*)-yl)butylthio)-4-(3,4-dichlorophenyl)-4*H*-1,2,4-triazol-3-yl)methyl)phenyl)-2,6-dichlorobenzenamine (33). Yellowish-green solid; R_f = 0.58 (DCM : MeOH 10 : 1); yield 49%; mp 191–197 °C. HPLC purity = 98.3% (C18 RP, acetonitrile/H_2O 97 : 3), TR = 15.8 min. ^{1}H NMR (400 MHz, DMSO-d6, ppm) δ: 7.70 (brs, 1H, NH), 7.52–7.49 (m, 4H, ArH), 7.41–7.39 (m, 1H, ArH), 7.31–7.26 (m, 3H, ArH), 7.21–7.19 (m, 2H, ArH), 7.11–7.08 (m, 4H, ArH), 6.94–6.89 (m, 4H, ArH), 4.34 (s, 2H, CH_2), 3.51 (t, 2H, J = 4.8 Hz, CH_2), 3.25 (t, 2H, J = 5.6 Hz, CH_2), 1.77–1.75 (m, 2H, CH_2), 1.45–1.43 (m, 2H, CH_2), ^{13}C NMR (100 MHz, DMSO-d6), δ. 167, 149.5, 143.8, 139.7, 137.2, 136.1, (132.8)2, (129.3)2, 128.9, 128.1, (127.7)3, 127.0, (126.9)2, 126.1, 125.8, 125.2, 124.9, 123.7, 123.0, 121.5, 118.7, 118.3, 117.8, 117.1, 114.3, 66.5, 49.3, 47.6, 37.5, 29.0, 28.1, 19.3. LC-MS: m/z = 736.57 $[M + H]^+$; analysis calculated for $C_{36}H_{27}Cl_4N_5S_2$. C, 58.78; H, 3.70; Cl, 19.28; N, 9.52; S, 8.72. Observed: C, 58.86; H, 3.68; N, 9.49.

3.9 General method for the synthesis of *N*-(4-acetylphenyl)-2-(2-(2,6-dichlorophenylamino)phenyl)acetamide (35)

The diclofenac **7** (10 mmol) were diluted in DCM 4 mL using an inert condition of nitrogen gas. Subsequent additions of *N*,*N*′-dicyclohexylcarbodiimide (DCC, 12 mmol), 1-hydroxy-benzotriazole (HOBt, 1.2 equiv.) and DMAP (2.5 equiv.) were performed and the was stirred for 5 minutes at normal laboratory temperature. 4-Amino acetophenone **34** (10 mmol) was added to the reaction and continued stirring at laboratory temperature for 12–16 h. After 24 h, the reaction was diluted with ethyl acetate and washed with aq. HCl (0.5 M, 20 mL). The extraction with ethyl acetate was repeated three times (50 mL each time). The three organic layers were combined and was added saturated sodium bicarbonate and brine (each 20 mL). The mixture was dried, filtered and the organic solvents were removed with reduced pressure of a rotary evaporator. The crude product **35** was purified by gravity column chromatography eluting with hexane and ethyl acetate solvent system.

3.10 General method for the synthesis (*E*)-*N*-(4-cinnamoylphenyl)-2-(2-(2,6-dichlorophenylamino)phenyl) acetamide (37)

Compound **37** was synthesized by stirring the mixture of ketone derivative **35**, (20 mmol) and para chlorobenzaldehyde (**36**, 20 mmol) in ethanol using piperidine as a base *via* Claisen Schmidt condensation reaction to yield chalcone based compound **37**.

3.11 General method for the synthesis of *N*-{4-[5-(4-chlorophenyl)-1-(4-sulfamoylphenyl)-4,5-dihydro-1*H*-pyrazol-3-yl]phenyl}-2-{2-[(2,6-dichlorophenyl)amino]phenyl}acetamide (39)

In 15 mL of ethanol, chalcones-based compound **37** (5 mmol) and 4-hydrazinyl benzene sulfonamide **38** (5 mmol) were stirred for two hours to obtain pyrazoline compound. When the reaction was completed, precipitate was formed, and recrystallization with ethanol afford compound **39**.

Yellow solid; R_f = 0.54 (DCM : MeOH 10 : 1); yield 48%; melting point 239–241 °C, HPLC purity = 99.1% (C18 RP, acetonitrile/H_2O 98 : 2), TR = 12.4 min. ^{1}H NMR (400 MHz, DMSO-d6, ppm) δ: ^{1}H NMR (400 MHz, DMSO-d6, ppm) δ: 9.51 (brs, 1H, NH), 8.12 (brs, 1H, NH), 7.90 (d, 2H, J = 8.4 Hz, ArH), 7.69 (d, 2H, J = 8.0 Hz, ArH), 7.61 (d, 2H, J = 8.4 Hz, ArH), 7.55 (d, 2H, J = 8.0 Hz, ArH), 7.40 (d, 2H, J = 7.6 Hz, ArH), 7.21 (d, 2H, J = 8.0 Hz, ArH), 7.16–7.12 (m, 4H, ArH), 7.09 (d, 2H, J = 8.0 Hz, ArH), 6.69 (d, 1H, J = 8.0 Hz, ArH), 5.98 (s, 2H, NH_2), 4.66 (dd, 1H, J = 11.7 Hz, 7.5 Hz, CH), 3.79 (s, 2H, CH_2), 3.41 (dd, J = 12.0 Hz, 17.4 Hz, 1H, CH), 2.89 (dd, J = 7.8 Hz, 17.1 Hz, 1H, CH); ^{13}C NMR (100 MHz, DMSO-d6), δ. 171.2, 152.3, 147.5, 142.5, 140.9, 139.4, 136.8, 133.1, 130.5, (129.1)4, (128.9)3, (128.4)2, (127.8)2, (127.4)2, (126.8)2, 126.2, (122.4)2, 121.5, 119.9, 118.1, (113.5)2, 54.4, 41.2, 32.5. LC-MS: m/z = 706.05 $[M + H]^+$; analysis calculated for $C_{35}H_{28}Cl_3N_5O_3S$. C, 59.62; H, 4.00; Cl, 15.09; N, 9.93; O, 6.81; S, 4.55. Observed value: C, 59.56; H, 4.02; N, 9.95.

3.12 *In vitro* enzyme inhibition studies

3.12.1 5-LOX inhibition assay. The assay was carried out by chemiluminescence method as reported in detail.[35] Briefly, a total of 100 μL reaction mixture contained 60 μL borate buffer, test compound, and 10 μL soybean 15-LOX enzyme solution. After pre-incubation for 5 min, 10 μL solution of luminol (3 nM) and cytochrome c (1 nM) was added per well and luminescence was measured by Synergy HTX, BioTek, USA plate reader. The reaction was initiated by 10 μL linoleic acid and chemiluminescence measured. Quercetin was used as a positive control. The active compounds were serially diluted and their percentage inhibitions were determined. This data was used for the computation of IC_{50} using Ez-Fit enzyme kinetics software (Perrella Scientific Inc. Amherst, USA). The percentage inhibition was calculated using following formula.

$$\text{Inhibition (\%)} = (\text{Abs of control} - \text{Abs of test comp}/\text{Abs of control}) \times 100$$

3.12.2 COX-2 inhibition assay. COX-2 (from human recombinant, Sigma Catalog Number C0858), lineolic acid (Sigma, CAS no 60-33-3), arachidonic acid (Sigma, Cat no 150384), *N*,*N*,*N*,*N*-tetramethyl-*p*-phenylenediamine dihydrochloride (Sigma, CAS 637-01-4), glutathione (Sigma, CAS 70-18-8), hematin (Sigma, CAS 15489-90-4). The cyclooxygenase 2 (300 units per ml) was activated for 5 minutes on ice with the additions of co-factor solution (50 μl, containing glutathione 0.9 mM, hematin 01 mM and *N*,*N*,*N*,*N*-tetramethyl-*p*-phenylenediamine dihydrochloride TMPD 0.24 mM) in Tris HCl buffer solution 0.1 M having pH of 8.0. Afterwards, enzyme solution (60 μl) and the synthesized compound's solution (20 μl, each compound's solution strengths were 31.25 to 1000 μg ml^{-1}) were kept for 5 minutes at normal laboratory temperature. The addition of arachidonic acid 30 mM, 570 nm using a double beam spectrophotometer. The percent enzymes inhibitions (COX-1 & 2) was calculated from the observed value of absorbance in a unit time. The IC_{50} values were calculated by plotting inhibitions value of each compound against its strength/concentration. The celecoxib and indomethacin were used standard drugs in cyclooxygenases assays.

3.12.3 *In vitro* AChE and BChE inhibition studies. *In vitro* bioassays were performed according to our previously reported procedure.[29] All the synthesized compounds assayed for their AChE (Electrophorous electricus type-VI-S, Sigma-Aldrich GmbH 4USA, code 1001596210) and BChE inhibition (Equine serum Lyophilized Sigma-Aldrich, code 101292670) by our previously reported modified Ellman's method using μQuant microplate spectrophotometer (MQX200, BioTek USA). Stock solution of the synthesized quinazoline was prepared with 0.1 M phosphate buffer (KH_2PO_4/K_2HPO_4) having of pH 8.0. Appropriate amount of DTNB (Ellman's reagent), quinazoline compounds, 0.03 U ml^{-1} of enzymes (AChE and BChE) were reacted by pre-incubating at 30 °C for 10 min and then further incubating for 15 min after addition of 1 mM ATCI or BTCI. Each reading was taken in triplicate and the IC_{50} values were obtained by plotting sample concentration verses the inhibition.

3.12.4 *In vitro* inhibition of MAO isoforms. The inhibitory action of the synthesized compounds was assessed employing commercially available recombinant human MAO-A and MAO-B (Thermo Fisher Scientific). The substrates for MAO-A and MAO-B were tyramine (MP Biomedicals, Inc.) and benzylamine, respectively. In a 96-well plate test plate, the protocol was carried out in the dark (Black). This was accomplished using the previously described fluorometric method.[25]

3.13 Blood–brain barrier (BBB) permeation assay

For the BBB penetration experiment, we used the PAMPA-BBB *in vitro* model. In this test, the synthesized compounds were dissolved in DMSO at a concentration of 10 mM and subsequently diluted with 100 M phosphate buffer at pH 7.4. The donor plate's filter membrane was coated with PBL in dodecane. The plate was then filled with 0.2 mL of test chemical solution. Similarly, the acceptor plate was filled with 0.2 mL of pH 7.4 PBS buffer and gently placed beneath the donor plate to form a "sandwich." For 20 hours, the plate was maintained at room temperature. The drug deliberation in acceptor, donor, and reference wells was observed using a UV plate reader. The synthesized compound's effective permeability (Pe) was calculated using the formula.[1]

$$\text{Pe} = [C \times \text{In}\ \{1 - ((\text{drug})\text{acceptor})/((\text{drug})\text{equilibrium})\}]$$

3.14 MTT assay for the evaluation of neurotoxicity

The MTT assay was used to examine the effect of the potent synthesized compounds on SH-SY5Y neuroblastoma cells (purchased from the ATCC). The SH-SY5Y cells were first cultivated in 96-well plates at a density of 1×10^5 cells per well in MEM/F12 supplemented with 10% fetal bovine serum, medium (200 μL), for one day at 37 °C under CO_2 (5 percent). The cells were then treated for 24 hours with varied doses of the test compounds (ranging from 1–40 μM). Following treatment of the cells with various doses of synthesized compounds and the standard, 20 μL of MTT reagent (5 mg mL^{-1}) was added to each well and incubated for 180 minutes at 37 °C (5 percent CO_2). Finally, under the microscope, the crystallization of a purple coloured precipitates were seen, which were solubilized by 1 mL of DMSO. The viability of the cells was measured using a microplate reader at 570 nm. The results were expressed as a percentage growth in each well in comparison to control cells cultivated without the standard/synthesized compounds.[2] The following equation was used to compute relative cell viability:

$$\text{Cell viability (\%)} = \text{(Abs. of sample)/(Abs. of control)} \times 100$$

3.15 *In vivo* acute toxicity studies

We followed the Ethical Guidelines for Animal Testing. Transgenic animals were purchased from the Jackson Laboratory USA; The Ethical Committee (Ref. No. DREC/20200405/06) of the Department of Pharmacy, University of Swabi, Pakistan, approved all the research protocols. The animals were euthanized humanely after the experimental protocol, following the AVMA Guidelines for the Euthanasia of Animals. To induce anaesthesia, the animals were slowly fed halothane fumes. The animals were euthanized as a result of the dosage and the prolonged time period.

Acute toxicity was determined by using our previously reported method.[35]

3.16 Docking studies

To explore the binding modes of newly synthesized compounds in the active site of LOX enzyme, all the compounds were docked into the binding pocket of COX-2, AChE and 15-LOX using Molecular Operating Environment (MOE). The crystal structure of human 15-lipoxygenase (15-LOXh) with PDB code 4NRE was downloaded from protein data bank. The protein structure was prepared using the preparation module of MOE and was subjected for 3-D protonation and finally was energy minimized to get a stable conformation of the target protein. All compounds were subjected to MOE for protonation and energy minimization using the default parameters (gradient: 0.05, Force Field: MMFF94X). The default parameters of MOE were used for molecular docking purpose, *i.e.*, Placement: Triangle Matcher, Rescoring-1: London dG, Refinement: Forcefield, Rescoring-2: GBVI/WSA. For each ligand total, ten conformations were allowed to generate, and the top-ranked conformations based on docking score were selected for protein-ligand interaction profile analysis. Ligand interaction and visualization was carried out *via* Pymol.

4 Conclusions

Present work described an extensive work to design a framework of multitarget scaffolds by using 3D crystal structures of the target enzymes. Continued with triazole **12** as lead compound, we modified it by considering the 3D structures and volumes of the active sites of target enzymes. The volume of active sites of AChE/BChE and MAO isoforms support bulky compounds for excellent inhibition. Hence in SAR study, incorporation of 3-methylene unit linkers resulted in loss of COX-2 inhibition. However, excellent inhibition and selectivity results towards eeAChE were obtained by increasing the linker length and with bulky scaffolds. Pyrimidine and pyrrolidine derivatives **28–31** inhibited eeAChE with a nanomolar concentration form 0.10 μM to 0.06 μM. Pyrazoline derivative **39** synthesized from modification of starting diclofenac **7** emerged as most potent eeAChE inhibitor ($IC_{50} = 0.03$ μM) and MAO-B inhibitor with IC_{50} value of 0.01 μM. All the biological active compounds were found to be non-neurotoxic. In a reversibility assay, all the studied active compounds showed reversibility and thus found to be devoid of side effects. In docking studies three-dimensional construction and interaction with key residues of all the studied biological macromolecules helped us to explain the experimental results.

Author contributions

UR conceived, designed, and supervised this study. He was involved in all the phases (from synthesis to pharmacological evaluation and manuscript writing/editing) that led to the completion of the manuscript. MAJ and SB synthesized the compounds. MAJ performed computational study and HPLC. *In vitro* and *in vivo* studies were supervised by AS and performed by MSJ. AZ and UF helped in pharmacological evaluation (*in vitro*) with AS and MSJ. MI performed cell viability/neurotoxicity assay and MAJ helped him. All the authors have read the manuscript and approved it for publication. The authors declare that there is no conflict of interest.

Conflicts of interest

There is no conflict of result between the authors.

Acknowledgements

Dr Umer Rashid (PI) is also thankful to Higher Education Commission (HEC) of Pakistan for the purchase of MOE 2016.0802 license under NRPU project (5291/Federal/NRPU/R&D/2016).

Notes and references

1 U. Rashid and F. L. Ansari, Challenges in designing therapeutic agents for treating Alzheimer's disease-From

serendipity to rationality, *Drug Design and Discovery in Alzheimer's Disease*, Elsevier, 2014, vol. 6, ch. 2, pp. 40–141.
2 M. Campora, C. Canale, E. Gatta, B. Tasso, E. Laurini, A. Relini, S. Pricl, M. Catto and M. Tonelli, *ACS Chem. Neurosci.*, 2021, **12**, 447–461.
3 B. P. Imbimbo and M. Watling, *Expert. Opin. Investig. Drugs*, 2019, **28**, 967–975.
4 Y. Xu, J. Zhang, H. Wang, F. Mao, K. Bao, W. Liu, J. Zhu, X. Li, H. Zhang and J. Li, *ACS Chem. Neurosci.*, 2018, **10**, 482–496.
5 M. A. Javed, N. Ashraf, M. Saeed Jan, M. H. Mahnashi, Y. S. Alqahtani, B. A. Alyami, A. O. Alqarni, Y. I. Asiri, M. Ikram, A. Sadiq and U. Rashid, *ACS Chem. Neurosci.*, 2021, **12**, 4123–4143.
6 H. Akıncıoğlu and İ. Gülçin, *Mini Rev. Med. Chem.*, 2020, **20**(8), 703–715.
7 K. Pape, R. Tamouza, M. Leboyer and F. Zipp, *Nat. Rev. Neurol.*, 2019, **15**(6), 317–328.
8 A. Webers, M. T. Heneka and P. A. Gleeson, *Immunol. Cell Biol.*, 2020, **98**(1), 28–41.
9 V. Calsolaro and P. Edison, *Alzheimer's Dementia*, 2016, **12**, 719–732.
10 L. J. Van Eldik, M. C. Carrillo, P. E. Cole, D. Feuerbach, B. D. Greenberg, J. A. Hendrix and K. K. Bales, *Alzheimer's Dementia*, 2016, **2**, 99–109.
11 O. Hidalgo-Lanussa, E. Baez-Jurado, V. Echeverria, G. M. Ashraf, A. Sahebkar, L. M. Garcia-Segura and G. E. Barreto, *J. Neuroendocrinol.*, 2020, **32**, e12776.
12 C. Patrono, *Br. J. Clin. Pharmacol.*, 2016, **82**(4), 957–964.
13 A. Zarghi and S. Arfaei, *Iran. J. Pharm. Res.*, 2011, **10**, 655–683.
14 R. G. Biringer, *Int. J. Environ. Res. Publ. Health*, 2019, **16**(14), 2560.
15 S. E. Desale and S. Chinnathambi, *J. Neuroinflammation*, 2020, **17**(1), 1–14.
16 J. C. Udeochu, J. M. Shea and S. A. Villeda, *Clin. Exp. Neuroimmunol.*, 2016, **7**(2), 114–125.
17 S. Manzoor and N. Hoda, *Eur. J. Med. Chem.*, 2020, **206**, 112787.
18 M. H. Elsherbeny, J. Kim, N. A. Gouda, L. Gotina, J. Cho, A. N. Pae, K. Lee, K. D. Park, A. Elkamhawy and E. J. Roh, *Antioxidants*, 2021, **10**, 1641.
19 S. Ilgın, D. Osmaniye, S. Levent, B. N. Sağlık, U. Acar Çevik, B. K. Çavuşoğlu, Y. Özkay and Z. A. Kaplancıklı, *Molecules*, 2017, **22**, 2187.
20 M. R. Bronzuoli, A. Iacomino, L. Steardo and C. Scuderi, *J. Inflamm. Res.*, 2016, **9**, 199.
21 A. Delgado, C. Cholevas and T. C. Theoharides, *Biofactors*, 2021, **47**, 207–217.
22 F. Zemek, L. Drtinova, E. Nepovimova, V. Sepsova, J. Korabecny, J. Klimes and K. Kuca, *Expet Opin. Drug Saf.*, 2014, **13**, 759–774.
23 P. Zhang, S. Xu, Z. Zhu and J. Xu, *Eur. J. Med. Chem.*, 2019, **176**, 228–247.
24 S. Ahmad, F. Iftikhar, F. Ullah, A. Sadiq and U. Rashid, *Bioorg. Chem.*, 2016, **69**, 91–101.
25 M. S. Nadeem, J. A. Khan and U. Rashid, *Int. J. Biol. Macromol.*, 2021, **193**, 19–26.
26 M. S. Nadeem, J. A. Khan, I. Kazmi and U. Rashid, *ACS Omega*, 2022, **7**(11), 9369–9379.
27 H. K. Askarani, A. Iraji, A. Rastegari, S. N. A. Bukhari, O. Firuzi, T. Akbarzadeh and M. Saeedi, *BMC Chem.*, 2020, **14**(1), 1–13.
28 C. Yamali, F. S. Engin, S. Bilginer, M. Tugrak, D. Ozmen Ozgun, G. Ozli and H. I. Gul, *J. Heterocycl. Chem.*, 2021, **58**(1), 161–171.
29 P. Sharma, A. Tripathi, P. N. Tripathi, S. S. Singh, S. P. Singh and S. K. Shrivastava, *ACS Chem. Neurosci.*, 2020, **11**, 2782.
30 A. Seth, P. A. Sharma, A. Tripathi, P. K. Choubey, P. Srivastava, P. N. Tripathi and S. K. Shrivastava, *Med. Chem. Res.*, 2018, **27**, 1206–1225.
31 L. Di, E. H. Kerns, K. Fan, O. J. McConnell and G. T. Carter, *Eur. J. Med. Chem.*, 2003, **38**(3), 223–232.
32 N. Augustin, V. K. Nuthakki, M. Abdullaha, Q. P. Hassan, S. G. Gandhi and S. B. Bharate, *ACS Omega*, 2020, **5**(3), 1616–1624.
33 C. F. Jin, Z. Z. Wang, K. Z. Chen, T. F. Xu and G. F. Hao, *J. Med. Chem.*, 2020, **63**(23), 15021–15036.
34 R. K. Tripathi, O. Goshain and S. R. Ayyannan, *ChemMedChem*, 2013, **8**(3), 462–474.
35 M. S. Jan, S. Ahmad, F. Hussain, A. Ahmad, F. Mahmood, U. Rashid, F. Ullah, M. Ayaz and A. Sadiq, *Eur. J. Med. Chem.*, 2020, **186**, 111863.5.